

# SPECTROSCOPY-BASED CHARACTERIZATION OF SINGLE WALL CARBON NANOTUBES

*M. Namkung<sup>1</sup>, J. S. Namkung<sup>2</sup>, B. Wincheski<sup>1</sup>, J. Seo<sup>3</sup> and C. Park<sup>4</sup>*

<sup>1</sup>*NASA Langley Research Center, Hampton, VA, USA 23681*

<sup>2</sup>*Naval Air Warfare Center, Patuxent River MD, USA 20670*

<sup>3</sup>*Hampton University, Hampton, VA, USA 23668*

<sup>4</sup>*National Institute of Aerospace, Hampton, VA, USA 23666*

We present the initial results of our combined investigation of Raman scattering and optical absorption spectroscopy in a batch of single wall carbon nanotubes (SWNTs). The SWNT diameters are first estimated from the four radial breathing mode (RBM) peaks using a simple relation of  $\omega_{RBM} = 248cm^{-1}nm / d_i(nm)$ . The calculated diameter values are related to the optical absorption peaks through the expressions of first interband transition energies, i.e.,  $E_{11}^S = 2a\gamma / d_i$  for semiconducting and  $E_{11}^M = 6a\gamma / d_i$  for metallic SWNTs, respectively, where  $a$  is the carbon-carbon bond length (0.144 nm) and  $\gamma$  is the energy of overlapping electrons from nearest neighbor atoms, which is 2.9 eV for a SWNT. This analysis indicates that three RBM peaks are from semiconducting tubes, and the remaining one is from metallic tubes. The detailed analysis in the present study is focused on these three peaks of the first absorption band by determining the values of the representative (n,m) pairs. The first step of analysis is to construct a list of possible (n,m) pairs from the diameters calculated from the positions of the RBM peaks. The second step is to compute the first interband transition energy,  $E_{11}$ , by substituting the constructed list of (n, m) into the expression of Reich and Thomsen, and Saito et al. Finally, the pairs with the energies closest to the experimental values are selected.

## 1. Introduction

The two integer coefficients, (n, m), of the lattice unit vectors of two-dimensional graphite unit cell define the chiral vector and, consequently, the chirality. It has been shown that the major physical properties of SWNTs are determined by the chirality [1, 2], and the determination of the (n,m) pair(s) of a single SWNT (batch of SWNTs) comprises a nearly complete morphology characterization. The (n, m) characterization of carefully prepared SWNT samples has been accomplished by a number of authors in the past [3]. The procedures employed for the previous work begin, first, to examine the radial breathing mode (RBM) Raman peak positions that correspond to the SWNT diameters through a simple expression of  $\omega_{RBM} = 248cm^{-1}nm / d_i(nm)$ . The diameter of a SWNT, however, is a multi-valued function of (n, m). In addition, one has to allow a reasonable degree of errors in the experiments.

Therefore, one normally establishes a list of possible (n, m) pairs by examining the Raman RBM peak positions. The subsequent steps involve detailed analysis to identify the most probable (n, m) pair from the list. This analysis is usually complex and the results can be subjective.

The present study is our first attempt to introduce a new method of determining the most probable pairs of (n, m) representing the chirality distribution in a batch of SWNTs. The unique element of this study is the inclusion of optical absorption spectroscopy. This technique directly measures the energies of interband transitions normally from three absorption bands, i. e., two for semiconducting and one for metallic tubes. In this study the analysis focuses on the details of three peaks in the first absorption band of semiconducting tubes in relation to the corresponding the Raman RBM peaks.

## 2. Experiments

The SWNT samples used in this study were synthesized by Carbon Nanotechnologies, Inc. through the HiPco process. A drop of SWNTs sonicated in water was deposited on an optically transparent plate and allowed to evaporate. The optical absorption spectra were obtained with a Cray Model 5E to collect data in a wide spectral range. A Digilab Fourier transform infrared (FT-IR) spectrometer with its resolution set to  $8 \text{ cm}^{-1}$  was used to measure the first absorption band from SWNTs. An AlmegaTM dispersive spectrometer, with a spectral resolution less than  $1.8 \text{ cm}^{-1}$ , was used with the laser wavelengths of 532 and 785 nm to obtain Raman spectra.

## 3. Results and discussion

Fig.1 shows a spectrum obtained from the dispersive Raman spectrometer with an incident laser beam of  $\lambda = 758 \text{ nm}$ . A spectrum obtained in this region with the incident laser beam of  $\lambda = 512 \text{ nm}$  shows the essentially the identical features. From the results in Fig. 1, we consider that those peaks at 268, 237, 232 and  $210 \text{ cm}^{-1}$  represent the major peaks in the tube diameter distribution of this batch of SWNTs. Using the expression of  $d_t(nm) = 248 \text{ cm}^{-1} nm / \omega_{RBM}$ , the corresponding tube diameters are calculated to be 0.925, 1.046, 1.069 and 1.187 nm. Applying  $E_{11}^S = 2a\gamma / d_t$ , the first interband transition energy in semiconducting SWNT, where  $a$  is the carbon-carbon bond length (0.144 nm) and  $\gamma$  is the energy of overlapping electrons from nearest neighbor atoms that is 2.9 eV in a SWNT,  $E_{11}$  values of 0.903, 0.798, 0.781 and 0.704 eV are obtained from the diameters calculated from the four RBM peaks of Fig. 1.

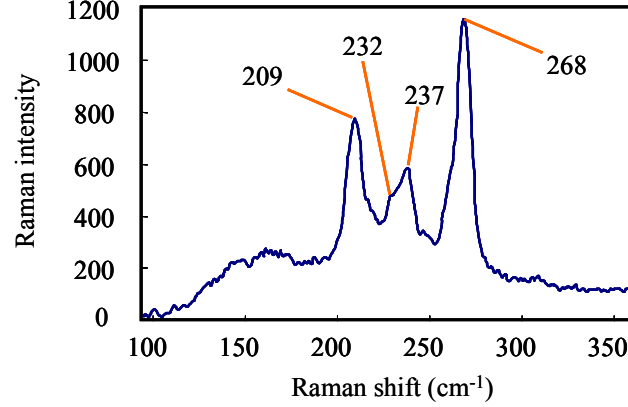


Figure 1. Breathing mode Raman scattering peaks obtained with an incident laser  $\lambda = 785$  nm.

Fig. 2 shows the first absorption band from the same sample using the FT-IR spectrometer. Three absorption peaks are found at 0.93, 0.84 and 0.8 eV. The absorption peak at 0.84 eV deviates from the computed values of 0.798 eV but those at 0.93 and 0.8 eV agree well with the computed values of 0.903 and 0.781 eV.

Fig. 3 shows the IR absorption spectrum obtained using Cray Model 5E dispersive spectrometer. The spectrum of Fig. 3 provides very useful information, i. e., the range of  $E_{11}^M$ , the first transition energy in a metallic tube, which is seen to be between 1.7 to 2.2 eV. This means that the RBM peak at  $210 \text{ cm}^{-1}$  corresponding to  $E_{11}^M = 6a\gamma/d_t = 2.11 \text{ eV}$  is well within the range of  $E_{11}^M$  in Fig. 3. Based on this, we conclude that three RBM peaks at 268, 237 and  $232 \text{ cm}^{-1}$  in Fig. 1 are from the semiconducting SWNTs and the one at  $210 \text{ cm}^{-1}$  is from the metallic SWNTs.

Using the expression  $d_t = (\sqrt{3}/\pi)a\sqrt{n^2 + m^2 + nm}$  and allowing an error range, a list of (n,m) pairs for each RBM peak is constructed. Table 1 provides a list of the calculated parameters for the RBM at  $268 \text{ cm}^{-1}$  by allowing a 5% error range. Two pairs, (2, 10) and (6, 7), are seen to produce the values of  $E_{11}^S$  that are closest to the measured one of 0.93 eV. The actual analysis in this work uses an error range of 15%. The second column shows the tube diameters corresponding to a given (n, m) pair. The third column provides  $E_{11}$  calculated using the expressions by Reich and Thomsen [5], and only the steps of application will be discussed.

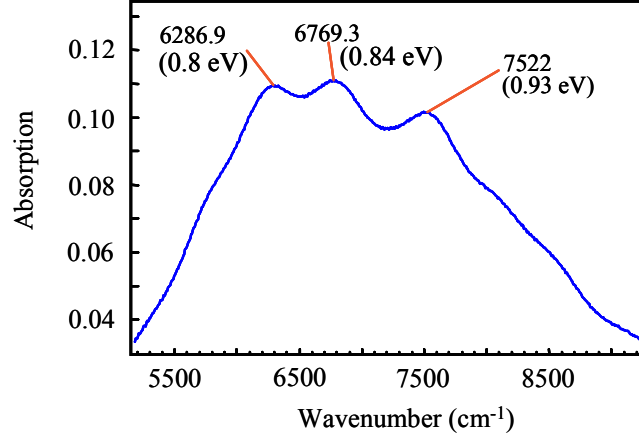


Figure 2. Three peaks in the first optical absorption band. The peak position at 0.84 eV deviates from the calculated value by 0.4 eV, but those of the other two peaks agree well with the calculated values.

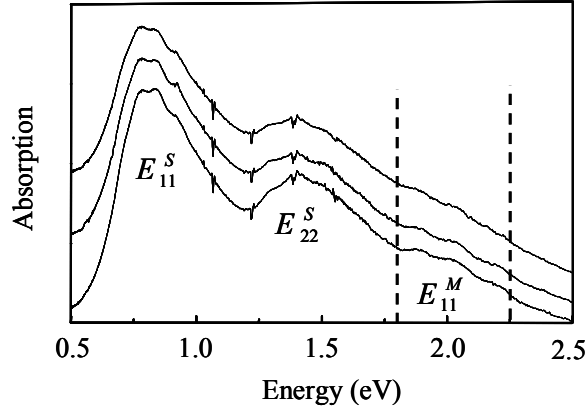


Figure 3. Optical absorption spectra collected from the SWNT sample at three different locations. These spectra provide important information on the range of  $E_{11}^M$  that is indicated by dotted vertical lines.

The allowed electron wave vector component perpendicular to the SWNT axis,  $k_T$ , is discrete due to the periodicity along the circumference, meanwhile that along the SWNT axis,  $k_z$ , is continuous. For given values of  $\pm k_T$ , the values of  $k_z$ s for which  $dE/dk_z$  vanishes, causing a Van Hove singularity in the density of states (DOS), are calculated. Two values of  $k_z$  result in two different energy values of singularity peaks for any SWNTs with an axial symmetry that is reduced from that of the armchair configuration, i. e.,  $n = m$ . These two

energies result in a split DOS peak structure. In the present work the energies for the split peaks are averaged since the experimental optical absorption peaks do not resolve the fine structures formed by the transitions among the split peaks. The values of  $E_{11}$  are calculated by using the nonzero minimum of  $k_T$  and the results are listed in the third column of Table 1. The fourth column lists the  $E_{11}$  values computed using  $E_{11}^S = 2a\gamma/d_t$  and  $E_{11}^M = 6a\gamma/d_t$  for semiconducting and metallic SWNTs, respectively, as given by Saito et al. We notice that for semiconducting SWNTs with,  $n - m \neq 3q$ , where  $q$  is an integer, the values of column 3 and 4 agree well. For metallic SWNT, satisfying the condition  $n - m = 3q$ , there is slight difference between the values of columns 3 and 4. As discussed earlier, the RBM peak at  $268 \text{ cm}^{-1}$  is identified as that from semiconducting SWNT, and, according to the results summarized in Table 1, (6, 7) is the most probable pair of (n, m) for the SWNTs producing this RBM peak.

Continuing the steps of analysis with the RBM peak found at  $237 \text{ cm}^{-1}$ , we find three pairs (n, m) resulting in  $E_{11}$  values close to the measured one of 0.84 eV as summarized in Table 2. The results for the RBM peak at  $232 \text{ cm}^{-1}$  are shown in Table 3. As clearly seen in these tables, several pairs of (n, m) result in  $E_{11}$  very close to the experimentally obtained value for a given RBM peak. It is therefore necessary to be able to analyze the second optical absorption band

Table 1. List of (n, m) pairs corresponding to the tube diameters within 5% of 0.925 nm computed from the RBM peak at  $268 \text{ cm}^{-1}$ . The third column shows the smallest  $E_{11}$  calculated for (n, m) using the expression by Reich and Thomsen. The fourth column lists  $E_{11}$  calculated using the expression by Saito et al. The pair (6, 7) gives the computed  $E_{11}$  value that is closest to the experimental values of 0.93 eV. The other pair (2, 10) is seen to produce a second closest  $E_{11}$  obtained using the expressions of (\*) Reich and Thomsen, and (\*) Saito et al. See text for more details.

n, m	diameter(nm)	$E_{11}$ (eV)*	$E_{11}$ (eV)**
0, 12	0.953	2.622	2.629
1, 11	0.952	0.912	0.915
<b>2, 10</b>	0.884	<b>0.944</b>	<b>0.945</b>
2, 11	0.963	2.284	2.602
3, 10	0.936	0.891	0.892
4, 9	0.916	0.91	0.912
5, 8	0.902	2.71	2.778
<b>6, 7</b>	0.895	<b>0.93</b>	<b>0.933</b>
6, 8	0.966	0.862	0.865
7, 7	0.963	2.539	2.602

Table 2. List of three (n, m) pairs for the RBM peaks  $237 \text{ cm}^{-1}$  that produce the  $E_{11}$  values close to the experimental value of 0.84 eV.

n, m	diameter(nm)	$E_{11}$ (eV)	$E_{11}$ (eV)
1, 12	0.995	0.839	0.84
5, 9	0.976	0.854	0.87
6, 8	0.966	0.862	0.865

Table 3. List of three (n, m) pairs for the RBM peaks  $232 \text{ cm}^{-1}$  that produce the  $E_{11}$  values close to the experimental value of 0.8 eV.

n, m	diameter(nm)	$E_{11}$ (eV)	$E_{11}$ (eV)
2, 12	1.041	0.802	0.802
5, 10	1.05	0.794	0.795
7, 8	1.03	0.807	0.809

for  $E_{22}^S$  to narrow down to a single most probable pair of (n, m) for each semiconducting SWNT RBM peak. Nevertheless, the critical element is to gain better understanding of the factors affecting the measurements, such as the effect of intertube interaction in a batch or bundles of SWNTs, which is estimated to increase the RBM peak position by as much as 10% from that of isolated tubes [6].

#### 4. Summary and conclusion

The results of present study clearly demonstrate that the feasibility of developing a simple method characterizing the representative (n, m) pairs of a batch of SWNT samples by combining the techniques of Raman scattering and IR absorption. To identify the true (n, m) pairs representing a batch of SWNTs, more progress in understanding of the effects of intertube interaction on the experiments and other potential factors is necessary.

#### References

1. See, for example, Carbon nanotubes, ed. Mildred Dresselhaus, Gene Dresselhaus and Phadeon Avon, Springer (Heidelberg, 2001).
2. R. Saito, G, Dresselhaus and M. S. Dresselhaus, Physical Properties of Carbon Nanotubes, Imperial College Press (London, 2001).
3. A. Jorio et al., Phys. Rev. Lett. **86**, 1118 (2001).
4. R. Saito, G, Dresselhaus and M. S. Dresselhaus, Phys. Rev. B. **61**, 2981 (2000).
5. S. Reich and C. Thomsen, Phys. Rev. B. **62**, 4273 (2000).
6. Henrad et al., Phys. Rev. B. **64**, 205403 (2001).